Colloid Journal, Vol. 67, No. 3, 2005, pp. 324–336. Translated from Kolloidnyi Zhurnal, Vol. 67, No. 3, 2005, pp. 363–376.

The Aggregation Work and Shape of Molecular Aggregates upon the Transition from Spherical to Globular and Cylindrical Micelles

M. S. Kshevetskiy and A. K. Shchekin

Fock Institute of Physics, St. Petersburg State University (Petrodvorets Branch), ul. Ul'yanovskaya 1, Petrodvorets, St. Petersburg, 198504 Russia

Received November 10, 2004

Abstract—The transition from spherical to globular and cylindrical equilibrium modifications of micelles in solutions of nonionic surfactants is numerically studied within the framework of the droplet model of molecular aggregates. Two branches of the curve of micelle aggregation work are plotted as a function of aggregation numbers. One of these curves corresponds to the globular micelles; the other, to spherocylindrical micelles. At aggregation numbers corresponding to the limiting spherical packing, both the globules and spherocylinders are transformed into the limiting sphere. It is shown that the ratio between the branches depends on the dimensionless parameter characterizing the ratio of electrostatic and surface contributions to the aggregation work. It is elucidated that, at certain values of this parameter and surfactant monomer concentration in solution, in addition to the maximum in the region of submicellar aggregates for spherical micelles, the second maximum arises on the curve of aggregation work as a function of aggregation numbers in the region of transition to spherocylindrical micelles. The appearance of an additional maximum is shown to be caused by the sum of surface, electrostatic, and concentration contributions to the aggregation work and is not directly related to the conformational contribution to the aggregation work.

INTRODUCTION

Micelles in aqueous surfactant solutions represent relatively stable molecular aggregates that are spontaneously formed from surfactant monomers. The micelle core is formed from densely packed hydrophobic fragments of surfactant molecules composed of hydrocarbon or carbon fluoride radicals. Polar groups (hereafter, we keep in mind a simpler case of nonionic surfactants whose polar groups do not form ions upon surfactant dissolution) appear on the boundary between the core and solution and form the electrical double layer.

Indicated features of micelle structure should be taken into account during the simulation of molecular aggregates in micellar solutions. One of commonly accepted models of molecular aggregate is the droplet model proposed by Tanford [1, 2] and elaborated in [3–10]. In this model, the aggregate core possesses the properties of apolar liquid and is characterized by the surface tension. This model was taken as a base model in [11, 12] when finding thermodynamic characteristics of micellization kinetics in surfactant solutions containing spherical micelles. In this case, the key thermodynamic parameter was the minimum work of aggregate formation (for brevity, aggregation work). The knowledge of this value allows us to determine the chemical potential of monomers in a spherical aggregate, equilibrium aggregate distribution over the aggregation numbers, and the heights of activation barriers of micelle formation and disintegration.

One of interesting and important property of micelles is their polymorphism, i.e., the existence of several stable equilibrium geometric forms of molecular aggregates [3, 7–10]. The basis of the analysis of various polymorphous modifications of micelles was laid in [3], where it was shown that the study of nonspherical micelles could also be based on the droplet model of molecular aggregate with invoking special condition called a packing factor. Using the analysis of various types of packing, one can conclude which micelle shapes can be realized depending on the geometric parameters of monomers [3, 7–10]. Note that limiting shapes of micelles corresponding to spheres, spherocylinders, and discs were commonly considered in the published literature; in some works devoted to the description of transitive shapes, significant simplifications were used. For example, in [3], the dense packing condition was applied only to the points of maximal curvature of aggregates that, in particular, made authors to conclude that, as the aggregation number increases, globular micelles were transformed into toroidal micelles. When studying the transition of spherical micelles to spherocylindrical micelles [13], the packing condition was satisfied by the choice of dumbbell model of a micelle with the spheres of limiting packing on its ends; the shape of neck and the part connecting spheres was determined by the minimization of aggregation work.

1061-933X/05/6703-0324

This work is devoted to the numerical study of equilibrium characteristics of nonspherical molecular aggregates in nonionic surfactant solutions upon the transition from spherical micelles to spherocylindrical and globular micelles. The study will be performed with account of the local packing condition and its relation to the value of local dipole moment on the surface of molecular aggregate. We also will study the conditions under which the second maximum in the region of transition to spherocylindrical micelles appears on the curve of aggregation work as a function of aggregation number, in addition to the maximum in the region of submicellar aggregates for spherical micelles.

1. DROPLET MODEL FOR NONSPHERICAL MOLECULAR AGGREGATES

Let us consider a nonspherical molecular aggregate formed in aqueous nonionic surfactant solution. For simplicity, we assume that, in solution, there is only one surfactant whose molecules have an unbranched hydrocarbon chain with dipole hydrophilic group at its end.

The number of carbon atoms in hydrocarbon chain of surfactant molecule is denoted by n_C. Let the end methyl group has volume v_S; methylene groups, volume v_C. Then, total volume v of hydrocarbon chain is equal to

$$v = v_S + (n_C - 1)v_C. \tag{1.1}$$

According to [1], at absolute solution temperature T = 273 K, $v_S \approx 54.3$ Å^3 and $v_C \approx 26.9$ Å^3.

Assuming that hydrocarbon chains of surfactant molecules are assembled into liquidlike compact hydrocarbon core (with no voids), we can consider such a molecular aggregate as a small hydrocarbon droplet with electrical dipoles of hydrophilic groups arranged on its surface. The aggregation number, i.e., the number of monomers in molecular aggregate, is denoted by n. At small aggregation numbers, the shape of corresponding aggregate will be spherical; then, for the aggregate core with radius R_m, we obtain

$$R_m = \sqrt[3]{\frac{3nv}{4\pi}}. \tag{1.2}$$

The possibilities of spherical packing of the aggregates are limited. The length of fully unfolded hydrocarbon chain of surfactant molecule is denoted by l_C. According to [1, 2], we have

$$l_C = (1.5 + 1.265n_C)\ \text{Å}. \tag{1.3}$$

It is evident that the radius R_m of aggregate spherical core with no voids cannot be larger than l_C; i.e., inequality

$$R_m \le l_C \tag{1.4}$$

takes place.

Further, assuming that polar groups are not densely packed on the aggregate surface, from Eqs. (1.2) and (1.4) we find aggregation number $n^{(sp)}$ corresponding to the limiting sphere with radius $R_m = l_C$

$$n^{(sp)} = \frac{4\pi l_C^3}{3v}. \tag{1.5}$$

Hereafter, we are interested only in the case when $n > n^{(sp)}$. Then, the molecular aggregate already cannot retain its spherical shape under the condition of the absence of voids and ought to acquire more complex configurations which will be described in next sections.

To calculate the formation work of molecular aggregate composed of n surfactant molecules, we take advantage of formula (2.12) in [11]. Extending this formula to the case of nonspherical micelles, we arrive at

$$W_n = \int_1^n w^{\beta\alpha} dn + \int_S \gamma dS - s_0\gamma n + k_B T n \ln(c^\alpha/c_1) + W_n^p + W_n^d, \tag{1.6}$$

where $w^{\beta\alpha}$ is the work needed to transfer surfactant molecules from solution to molecular aggregate in the absence of pressure and surface tension with allowance for hydrophobic effect; γ is the surface tension of aggregate hydrocarbon core; S is the surface area of aggregate core; s_0 is the cross-sectional area of polar group on the surface of aggregate core; k_B is Boltzmann's constant; c^α and c_1 are the concentrations of hydrocarbon tails in aggregate core and of surfactant molecules in solution, respectively; W_n^p is the contribution from the interactions of polar groups on aggregate surface; and W_n^d is the conformational contribution related to the bending of the hydrocarbon tails of surfactant molecules in an aggregate.

We comment the first and last two terms in formula (1.6) in more detail. For the sufficiently long chains composed of large numbers of hydrocarbon segments ($n_C \gg 1$), according to [1, 2], we have the following empirical expression for work $w^{\beta\alpha}$:

$$w^{\beta\alpha} = -Bn_C, \tag{1.7}$$

where B is a positive constant. Positive B value implies the hydrophobicity of hydrocarbon groups; hence, the first term in Eq. (1.6) is called hydrophobic contribution. According to empirical data reported in [1, 2, 9], at temperature close to 20°C, constant $B \approx 1.4k_BT$. Note also that, according to Eqs. (1.6) and (1.7), hydrophobic contribution is linear with respect to n.

The appearance of conformational contribution W_n^d in the formation work is associated with the fact that, when packing in the aggregate core, hydrocarbon segments of surfactant molecules have the conformation that is different than their conformation in hydrocarbon phase. Using results reported in [8, 10], we write W_n^d as

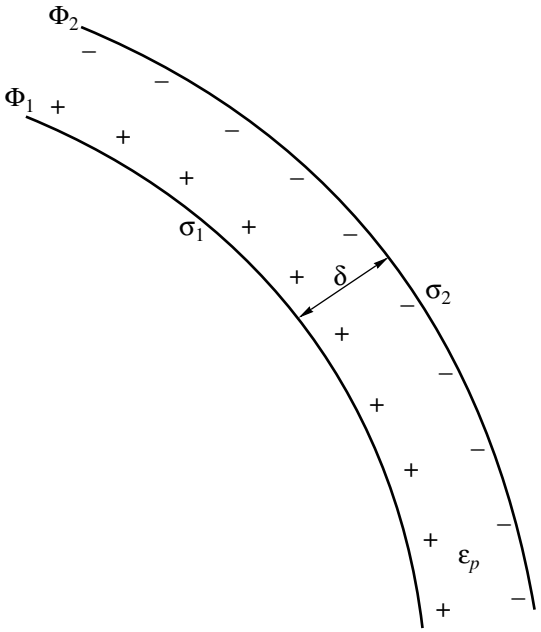

Fig. 1. Double electrical layer on the surface of surfactant molecular aggregate.

$$W_n^{\mathrm{d}} = k_{\mathrm{B}}T\frac{\pi^2 AN}{80l_{\mathrm{C}}^2}n, \tag{1.8}$$

where N is the number of rigid segments in the hydrophobic fragment of surfactant molecule, and the value of A depends on the aggregate shape and has the dimension of surface area. For a spherical aggregate, $A = 3R_{\mathrm{m}}^2$; for infinite cylinder, $A = 5R_{\mathrm{c}}^2$ (R_{c} is the cylinder radius), and, finally, for infinitely extended layer, $A = (5/2)H^2$ (H is the layer thickness). In the case of hydrophobic fragments composed of methylene groups, according to [10], rigid segment consists, on the average, of 3.6 such groups so that $N = n_{\mathrm{C}}/3.6$.

In the situations when the aggregate profile slightly differs from one of aforementioned configurations, corresponding contribution can be generalized. For example, it was done for the cylindrical portion of dumbbell micelle. For the aggregates of arbitrary shape, it is impossible to write the explicit form of conformational contribution. Estimating this contribution for aggregates of spherical, cylindrical, and planar shapes, we obtain

$$W_n^{\mathrm{d}} \lesssim k_{\mathrm{B}}TB_A n n_{\mathrm{C}}, \tag{1.9}$$

where $B_A = 0.1$ for the sphere, 0.17 for infinite cylinder, and 0.3 for infinitely large layer. Further, estimating ratio $W_n^{\mathrm{d}}/(w^{\beta\alpha}n)$ with account of Eqs. (1.9) and (1.7), we can seen that the conformational contribution is rather small compared to the hydrophobic contribution and can be ignored.

Let us now estimate contribution W_n^{p} from polar groups. The approach of polar groups upon an increase in the aggregation numbers and packing of hydrocarbon tails inside of molecular aggregate leads to their interaction which is predominantly contributed by the mutual electrostatic repulsion of dipoles. Let us denote corresponding electrostatic contribution to work W_n by W_{el} and assume that

$$W_n^{\mathrm{p}} = W_{\mathrm{el}}. \tag{1.10}$$

Because the formation of molecular aggregates in solution occurs at constant temperature and external pressure, W_{el} represents Gibbs electrostatic energy. Then, to find W_{el}, we can use formula

$$W_{\mathrm{el}} = \frac{1}{8\pi}\int_{\Upsilon}\mathbf{E}\mathbf{D}d\mathbf{r}, \tag{1.11}$$

where $\mathbf{E}$ and $\mathbf{D}$ are the vectors of strength and induction of electric field, respectively, and the integration is performed with respect to entire volume Υ that does not include the sources of electric field (in the case under consideration, these are the dipoles in the double layer on the aggregate surface).

Let us transform the expression for W_{el} into the integral over the aggregate surface. Using relation $\mathbf{E} = -\nabla\Phi$ for electric field potential Φ, Laplace's equation $\Delta\Phi = 0$, and boundary condition $D_n = -4\pi\sigma$ connecting the normal component of electric field induction D_n with of the density σ of charge distribution on surface S, we obtain (see Fig. 1)

$$W_{\mathrm{el}} = \frac{1}{2}\int_{S_1}\sigma_1\Phi_1 dS_1 + \frac{1}{2}\int_{S_2}\sigma_2\Phi_2 dS_2, \tag{1.12}$$

where subscripts 1 and 2 denote the values related to the inner and outer shells of electrical double layer, respectively.

Taking into account that electrical double layer is formed from the dipole groups of surfactant molecules, we arrive at the local electroneutrality condition, $\sigma_1 dS_1 = -\sigma_2 dS_2$. Then, expression (1.12) for contribution W_{el} can be represented as

$$W_{\mathrm{el}} = \frac{1}{2}\int_{S_1}\sigma_1(\Phi_1 - \Phi_2)dS_1. \tag{1.13}$$

For the local difference of potentials $\Phi_1 - \Phi_2$, we use the formula of flat capacitor (this is possible when the thickness of double layer δ is markedly smaller than the curvature radius of hydrocarbon core). This condition is admissible for nonionic surfactants; for zwitterionic surfactants, this condition can be fulfilled only at the limit. Correspondingly, we obtain

$$\Phi_1 - \Phi_2 = \frac{4\pi\sigma_1}{\varepsilon_p}\delta, \tag{1.14}$$

where ε_p is the permittivity of inner space of the double layer. Assuming that dipoles forming double layer are oriented normally toward the surface of hydrocarbon core and, hence, thickness δ of the layer is constant, we represent Eq. (1.13), with allowance for Eq. (1.14), as

$$W_{el} = \frac{2\pi}{\varepsilon_p \delta}\int_S \sigma_p^2 dS, \quad (1.15)$$

where $\sigma_p = \sigma_1\delta$ is the local density of the dipole moment on the surface of aggregate core.

In [1, 3, 8, 13], to describe electrostatic contribution, formula

$$W_{el} = \int \frac{B_p}{s} dn \quad (1.16)$$

was used, where B_p is the proportionality coefficient depending on the characteristics of solution and surfactant molecules and s is the surface area of hydrocarbon core per surfactant molecule in a micelle. In view of the complexity of this problem, main attention was focused on the relatively simple cases. For example, it was assumed in [3, 8] that polar groups are packed densely on the micelle surface. This meant that $s = s_0 = \text{const}$; then, contribution W_{el} appeared to be the known in advance linear function of aggregation number n. In [11], micelles with simple configurations were considered for which integral (1.16) could be calculated analytically. More complex cases virtually were not studied.

2. AGGREGATION WORK AS A FUNCTIONAL OF THE PROFILE OF AGGREGATE SURFACE

To find the equilibrium profile of aggregate surface, it is necessary to minimize expression (1.6) for aggregation work W_n. In accordance with the Gibbs–Curie generalized principle for micelles [9] (assuming that micelle concentration is still low and the contribution of Brownian rotation is negligibly small), we search for the minimum under the condition of constant volume V of aggregate core. Assuming that the core is incompressible, we have

$$\int_V dV = nv. \quad (2.1)$$

Condition (2.1) automatically means that aggregation number n is also constant. Therefore, aggregation number-dependent contributions [linear with respect to n in Eq. (1.6)] to formation work W_n will not affect the equilibrium profile of aggregate surface with given n. According to Eqs. (1.7) and (1.6), among such contributions is the larger (by the absolute value) hydrophobic contribution, whose role in the aggregation work at varying n is very significant.

Omitting contributions in Eq. (1.6), which are constant at given n, for aggregate shape-dependent part W of the aggregation work, which further will be minimized, we have

$$W = W_s + W_{el}, \quad (2.2)$$

where $W_s \equiv \int_S \gamma dS$ is the work that is needed to create the surface of molecular aggregate nucleus and that is responsible for the surface contribution to the total aggregation work in Eq. (1.6). Thus, only two contributions, electrostatic and surface, compete for the definition of micelle equilibrium shape.

In order to find electrostatic contribution W_{el} to the work of aggregate formation in relation (1.15), it is necessary to determine the dipole moment of unit surface area σ_p. Let us represent the aggregate as a closed monolayer whose hydrocarbon interlayer thickness l is no more than the length of hydrocarbon tail of surfactant molecule. Let us consider the element of such a monolayer shown in Fig. 2 [7]. Suggesting that the surface of hydrocarbon core is not too curved so that the thickness of hydrocarbon interlayer does not exceed principal curvature radii R_1 and R_2 of the surface core, one can write simple geometric relation between surface area $dS = R_1R_2d\theta_1d\theta_2$ of the element of hydrocarbon core surface (θ_1 and θ_2 are the element angles in principal cross sections) and volume dV of the element of hydrocarbon core

$$\begin{aligned} dV &= d\theta_1 d\theta_2 \int_0^l (R_1 - l')(R_2 - l')dl' \\ &= d\theta_1 d\theta_2 [R_1R_2 l - (R_1 + R_2)l^2/2 + l^3/3], \end{aligned} \quad (2.3)$$

where the integration with respect to thickness is performed along the normal to the core surface. Specifying the differential of surface dS, we rewrite Eq. (2.3) as

$$\frac{dV}{dS} = l\left[1 - \frac{l}{2}\left(\frac{1}{R_1} + \frac{1}{R_2}\right) + \frac{l^2}{3R_1R_2}\right]. \quad (2.4)$$

Relation (2.4) is called the packing equation [3]. In the case of dense packing of polar groups, surface area S of the aggregate core will be determined by relation $S = s_0n$. Then, with account of Eq. (2.1), we have

$$\frac{dV}{dS} = \frac{vdn}{s_0dn} = \frac{v}{s_0} = \text{const}, \quad (2.5)$$

where dn is the number of surfactant molecules per volume dV. From relations (2.4) and (2.5) and condition $l \le l_C$, we find conditions under which the packing of polar groups on the aggregate surface is not dense. In the case of spherical shape ($R_1 = R_2 \le l_C$), we have $s_0 \le 3v/l_C$; for cylindrical configuration ($R_1 \le l_C$, $R_2 = \infty$), we obtain $s_0 \le 2v/l_C$; finally, for the flat configuration ($R_1 = R_2 = \infty$), we arrive at $s_0 \le v/l_C$. Combining these results, we can represent the condition of loose packing of polar groups on the aggregate surface as

$$s_0 \leqslant v/l_C. \quad (2.6)$$

Further, recalling that $dV = vdn$ and for the total dipole moment of the surface that rests on the same volume,

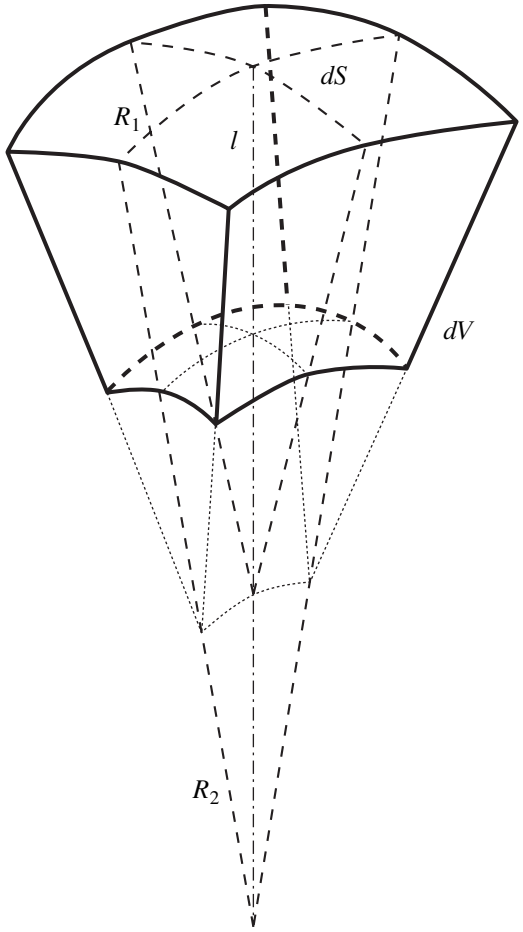

Fig. 2. The element of a monolayer with thickness *l,* volume *dV*, and base surface area *dS*. Principal curvature radii R_1 and R_2 are denoted by solid dashed lines.

equality $pdn = \sigma_p dS$ (where p is the dipole moment of a surfactant molecule) takes place, we obtain

$$\frac{dV}{dS} = \frac{v}{p}\sigma_p. \tag{2.7}$$

Substituting Eq. (2.4) into (2.7), we arrive at the next relation for the dipole moment σ_p of aggregate unit surface

$$\sigma_p = \frac{pl}{v}\left[1 - \frac{l}{2}\left(\frac{1}{R_1} + \frac{1}{R_2}\right) + \frac{l^2}{3R_1R_2}\right]. \tag{2.8}$$

For the micelles with aggregation number $n < n^{(sp)}$, the thickness l of hydrocarbon interlayer is equal to radius R_m of micelle core. The l value increases with the aggregation number and, at $n = n^{(sp)}$, the thickness l of hydrocarbon layer will be maximal, $l = l_C$. Further increase of the l value is impossible, hence, for micelles with $n > n^{(sp)}$, we assume that l will be constant over the entire monolayer surface and equal to its maximal value (i.e., $l = l_C$).

In order to write final expression for desired work W as a functional of the profile of aggregate surface at $n \geq n^{(sp)}$, we should take into account Eqs. (1.15) and (2.8), as well as equality $l = l_C$. Then, from Eq. (2.2), we obtain

$$W = \gamma\int_S \left\{1 + \frac{2\pi p^2 l_C^2}{\gamma\delta\varepsilon_p v^2} \times \left[1 - \frac{l_C}{2}\left(\frac{1}{R_1} + \frac{1}{R_2}\right) + \frac{l_C^2}{3R_1R_2}\right]^2\right\} dS. \tag{2.9}$$

Note that, when deriving Eq. (2.9), we used condition (2.1) of constant volume V of the aggregate and the condition of dipole orthogonality to the surface of molecular aggregate ensuring the equality

$$\int_S \sigma_p dS = np, \tag{2.10}$$

which, with allowance for Eq. (2.8) and condition $l = l_C$, can be rewritten as

$$\int_S \left[1 - \frac{l_C}{2}\left(\frac{1}{R_1} + \frac{1}{R_2}\right) + \frac{l_C^2}{3R_1R_2}\right] dS = \frac{nv}{l_C}. \tag{2.11}$$

Conditions (2.1) and (2.11), together with expression (2.9), present the total system of relations needed for finding the equilibrium profile of the surface of molecular aggregate and corresponding minimal aggregation work of micelle. The dependence of the aggregate shape is ensured by the presence of principal curvature radii R_1 and R_2 in Eqs. (2.11) and (2.9).

Since the domain of applicability of relations (2.9) and (2.11) is limited by condition $n \geq n^{(sp)}$, for spherical aggregates at $n < n^{(sp)}$, we use results obtained in [11]. In particular, for total aggregation work W_n of spherical molecular aggregate as a function of aggregation numbers n with the disregard for conformational contribution in [11], we can write simple analytical formula

$$W_n = b_1 n^{4/3} - b_2 n + b_3 n^{2/3}, \tag{2.12}$$

where b_1, b_2, and b_3 are the coefficients of electrostatic contribution (proportional to $n^{4/3}$), the sum of hydrophobic and concentration contributions (proportional to n), and surface contribution (proportional to $n^{2/3}$), respectively. In our notations, these coefficients have the following form:

$$b_1 = \frac{p^2}{3\varepsilon_p\delta}\sqrt[3]{\frac{6\pi^2}{v^2}}, \quad b_2 = Bn_C + s_0\gamma + k_BT\ln\frac{c_1}{c^\alpha}, \quad b_3 = \gamma\sqrt[3]{36\pi v^2}. \tag{2.13}$$

Evidently, at $n = n^{(sp)}$, the relation for the aggregation work of nonspherical molecular aggregate should

be transformed into formula (2.12). Comparing Eqs. (2.12) and (2.2), we see that the transition from reduced functional W to total aggregation work W_n can be performed by formula

$$W_n = W - b_2 n. \tag{2.14}$$

3. DIMENSIONLESS PARAMETERS OF A PROBLEM OF THE MINIMIZATION OF AGGREGATION WORK

To solve the problem of finding aggregate shape ensuring the minimum of aggregation work W, we pass to spherical coordinate system with the origin in the center of aggregate mass. We choose the direction of azimuth axis coinciding with the aggregate symmetry axis and use variable $x \equiv \cos\theta$ instead of azimuth angle θ.

The profile of aggregate surface is denoted by $a(x)$. Dimensionless parameters and the values of the problem of the minimization of aggregation work are determined by relations

$$\kappa \equiv \frac{2\pi p^2 l_C^2}{\gamma \delta \varepsilon_p v^2}, \quad \tilde{V} \equiv \frac{3nv}{4\pi l_C^3},$$
$$\tilde{a}(x) \equiv \frac{a(x)}{l_C}, \quad \tilde{R}_{1,2} \equiv \frac{R_{1,2}}{l_C}, \quad \tilde{W} \equiv \frac{W}{4\pi\gamma l_C^2}. \tag{3.1}$$

It is evident that parameter κ characterizes the ratio of electrostatic and surface contributions to the aggregation work (this ratio, at $n = n^{(sp)}$, is equal to $\kappa/9$), $\tilde{V}$ is the dimensionless aggregate volume, $\tilde{a}(x)$ is the dimensionless aggregate profile, $\tilde{R}_{1,2}$ are the dimensionless principal curvature radii, and $\tilde{W}$ is the dimensionless aggregation work. Using definitions (3.1) and accounting for the profile symmetry $a(x) = a(-x)$, we rewrite functional (2.9) and conditions (2.1) and (2.11) in the form

$$\tilde{W} = \int_0^1 \left\{ 1 + \kappa \left[1 - \frac{1}{2}\left(\frac{1}{\tilde{R}_1} + \frac{1}{\tilde{R}_2} \right) + \frac{1}{3\tilde{R}_1\tilde{R}_2} \right]^2 \right\} \times \tilde{a}\sqrt{\tilde{a}^2 + (1-x^2)\tilde{a}_x^2}\,dx, \tag{3.2}$$

$$\tilde{V} = \int_0^1 \tilde{a}^3 dx, \tag{3.3}$$

$$\frac{\tilde{V}}{3} = \int_0^1 \left[1 - \frac{1}{2}\left(\frac{1}{\tilde{R}_1} + \frac{1}{\tilde{R}_2} \right) + \frac{1}{3\tilde{R}_1\tilde{R}_2} \right] \times \tilde{a}\sqrt{\tilde{a}^2 + (1-x^2)\tilde{a}_x^2}\,dx, \tag{3.4}$$

where, according to [14], the dependence of $\tilde{R}_{1,2}$ on x in the chosen coordinate system is determined as

$$\tilde{R}_1 = \frac{[\tilde{a}^2 + (1-x^2)\tilde{a}_x^2]^{3/2}}{\tilde{a}(\tilde{a} + x\tilde{a}_x) + (1-x^2)(2\tilde{a}_x^2 - \tilde{a}\tilde{a}_{xx})},$$
$$\tilde{R}_2 = \frac{\tilde{a}[\tilde{a}^2 + (1-x^2)\tilde{a}_x^2]^{1/2}}{\tilde{a} + x\tilde{a}_x}. \tag{3.5}$$

It is seen that the solution of a problem of minimization of $\tilde{W}$ depends on two parameters, κ and $\tilde{V}$. It is easy to note that, at $\tilde{V} = 1$, there is a trivial solution: $\tilde{a}(x) = 1$. This solution corresponds to the limiting sphere, i.e., the sphere with radius $R_m = l_C$.

Let us represent micelle profile $\tilde{a}(x)$ as an infinite series in powers of Legendre polynomial $P_n(x)$. With account of symmetry, we have

$$\tilde{a}(x) = \sum_{i=0}^{\infty} \tilde{a}_i P_{2i}(x). \tag{3.6}$$

The substitution of this expression into expressions (3.2)–(3.5) reduces the problem of minimization of the functional $\tilde{W}[\tilde{a}(x); \kappa, \tilde{V}]$ to the problem of the minimization of corresponding function $\tilde{W}(\tilde{a}_0, \tilde{a}_1, \ldots; \kappa, \tilde{V})$. Assuming that series (3.6) is converged and the contribution from higher terms of a series is negligible, we cut-off series (3.6) at a certain $i = N$. In other words, we assume that $\tilde{a}_i = 0$ at $i \geq N$. From the formal viewpoint, such an operation can be considered as the parameterization of profile $\tilde{a}(x)$ using the finite number of parameters $\tilde{a}_0, \tilde{a}_1, \ldots, \tilde{a}_{N-1}$. Thus, the problem is reduced to the minimization of function $\tilde{W}(\tilde{a}_0, \tilde{a}_1, \ldots, \tilde{a}_{N-1}; \kappa, \tilde{V})$ provided that two supplementary conditions are present. Now, the unknown parameters are $\tilde{a}_0, \tilde{a}_1, \ldots, \tilde{a}_{N-1}$, values κ and $\tilde{V}$ act as additional parameters, and parameter N controls the accuracy of approximation.

Let us choose the initial approximation. The analysis of a problem shows that, in this case, we cannot use approximation $\tilde{a}(x) = 1$ corresponding to the sphere as a starting solution to the numerical scheme. This is explained by several reasons. First, at $\tilde{V} \longrightarrow 1 + 0$, Eqs. (3.3) and (3.4) become almost linearly dependent. In particular, this implies that the solution cannot be constructed by the expansion into series in powers of small parameter characterizing the deviation from the sphere. Second, as will be shown later, in the vicinity of $\tilde{V} = 1$, there are two different types of solution. At $\tilde{V} \longrightarrow 1 + 0$, both solutions tend to the sphere; moreover, the domain of attraction narrows for each solution. This results in the instability of the operation of numerical method in the indicated vicinity; hence, lim-

iting transition $\tilde{V} \longrightarrow 1 + 0$ cannot be realized in practice.

To solve this problem, we used slightly flattened (at the poles) sphere with volume $\tilde{V} \approx 1.1$ as an initial approximation. This approximation (after its refinement) was used as a starting one for finding globular micelles. Such micelles are understood as stable aggregates whose shape resemble flattened (at the poles) sphere which is transformed into disc with an increase in size. When considering solutions of another type, it turned out that it is more convenient to start with larger sizes; in this case, fairly large cylinder of volume $\tilde{V} \approx$ 4–5 with cross-sectional radius $\tilde{R} = 1$ and hemispherical ends was used as an initial approximation. This approximation (after its refinement) was used as a starting one for finding spherocylindrical micelles. Such micelles are understood as elongated cylindrical aggregates with rounded ends; they are often called spherocylinders. Further, for finding the dependence of micelle formation work as a function of aggregation numbers, we used solutions obtained at the preceding step of iteration process.

It is necessary to clarify the transition of globular micelles to disc-like ones. It was shown [3] that, in the case of dense packing, globular micelles should be transformed into toroidal. Figure obtained by the rotation of ellipse around the axis that is parallel to its symmetry axis was considered as the shape of a micelle. In order to find ellipse parameters, the conditions of constant packing and surface area of a micelle, as well as packing condition, which was applied only to the points of maximum curvature profile, were used in [3]. Main disadvantages of this model are profile nonsmoothness at the poles and the violation of local packing conditions. It is these events that resulted in the transition of globular micelles to toroidal.

4. NUMERICAL PROCEDURES FOR FINDING THE PROFILE OF NONSPHERICAL MICELLE

As was shown above, the considered problem of finding equilibrium profiles of molecular aggregates can be reduced to the problem of the minimization of function $\tilde{W}(\tilde{a}_0, \tilde{a}_1, \ldots, \tilde{a}_{N-1}; \kappa, \tilde{V})$ with the presence of supplementary conditions in the form

$$Y_{1,2}(\tilde{a}_0, \tilde{a}_1, \ldots, \tilde{a}_{N-1}; \kappa, \tilde{V}) = 0. \quad (4.1)$$

Such a problem can be solved using two procedures. When using Lagrange multiplier method, this problem is reduced to the following system of nonlinear equations:

$$\frac{\partial}{\partial \tilde{a}_j}\left[\tilde{W}(\tilde{a}_0, \tilde{a}_1, \ldots, \tilde{a}_{N-1}; \kappa, \tilde{V}) + \sum_{i=1}^{2} \zeta_i Y_i(\tilde{a}_0, \tilde{a}_1, \ldots, \tilde{a}_{N-1}; \kappa, \tilde{V})\right] = 0, \quad (4.2)$$

$$j = 0, 1, \ldots, N-1,$$

$$Y_{1,2}(\tilde{a}_0, \tilde{a}_1, \ldots, \tilde{a}_{N-1}; \kappa, \tilde{V}) = 0.$$

Here, unknown values are $\tilde{a}_0, \tilde{a}_1, \ldots, \tilde{a}_{N-1}$ and Lagrange multipliers ζ_1 and ζ_2. The system consisted of $N + 2$ equations with $N + 2$ unknowns and two additional parameters can be rewritten as

$$F_i(\boldsymbol{\xi}, \mathbf{z}) = 0, \quad i = 1, \ldots, N+2, \quad (4.3)$$

where F_i represent the left-hand sides of equations in (4.2), $\boldsymbol{\xi} = (\tilde{a}_0, \tilde{a}_1, \ldots, \tilde{a}_{N-1}, \zeta_1, \zeta_2)$ are the unknown values, and $\mathbf{z} = (\kappa, \tilde{V})$ is the set of independent parameters. We solve this system minimizing the residual by Newton's method [15]. For this purpose, we determine residual vector $\mathbf{F} = (F_1, \ldots, F_{N+2})$ and represent system (4.3) as $\mathbf{A}\boldsymbol{\xi} = 0$, where $\mathbf{A}$ is the nonlinear operator corresponding to the set of equations (4.3).

Let us now describe the iteration procedure. At the first step, we have an initial approximation $\boldsymbol{\xi}_0$. We calculate $\mathbf{F}_0 = \mathbf{A}\boldsymbol{\xi}_0$ and matrix $\mathbf{J}_{ij}^0 = \partial(\mathbf{A}\boldsymbol{\xi})_i/\partial\xi_j$ in point $\boldsymbol{\xi} = \boldsymbol{\xi}_0$. We find next approximation $\boldsymbol{\xi}_1 = \boldsymbol{\xi}_0 + \Delta\boldsymbol{\xi}$ using equation $\mathbf{J}_0\Delta\boldsymbol{\xi} = -\mathbf{F}_0$. This procedure is repeated until the required accuracy is achieved.

Then, slightly varying one of components of vector $\mathbf{z}$, using the resultant solution as a starting initial approximation, and repeating the procedure of system solution, we find the dependences of equilibrium profile and thermodynamic characteristics of a micelle on this parameter; the resultant dependences can represented as plots.

Note that the accuracy of solution can be controlled by several methods. The simplest method is to use smallness of $|\mathbf{F}|$. This estimate demonstrates how well the modified system of equations (4.3) is solved. One can use the smallness of correction $|\Delta\boldsymbol{\xi}|$. This allows us to estimate how reasonable is to continue the calculations. One can also substitute found vector $\boldsymbol{\xi}$ into the initial system of equations and take a look how much the found solution differs from the true one. For example, when approaching the boundary of the applicability of numerical method, the first estimate begins to increase, whereas the second and third estimates can remain small. An increase of the second estimate states the deterioration of the quality of initial approximation. An increase of the third estimate demonstrates that the chosen number of parameters N is not large enough. Note that the described method will adequately converge, if the initial approximation lies in the vicinity of solution.

In the case, when the initial approximation is unsatisfactory to approach the root rather closely, one can use the modified method of gradient descent. Classical

method of gradient descent in inapplicable in this case due to supplementary conditions (4.1). For simplicity, let us consider the modified gradient descent method in the situation, where there is only one supplementary condition. Let us now determine vector $\boldsymbol{\xi}$ as $\boldsymbol{\xi} = (\tilde{a}_0, \tilde{a}_1, \ldots, \tilde{a}_{N-1})$. Then, at the first step, we have initial approximation $\boldsymbol{\xi}_0$. Further, we calculate residual $Y_1^0 = Y_1$ and vectors $(\nabla \tilde{W})_j^0 = \partial \tilde{W}/\partial \xi_j$ and $(\nabla Y_1)_j^0 = \partial Y_1/\partial \xi_j$ at point $\boldsymbol{\xi} = \boldsymbol{\xi}_0$. Next approximation $\boldsymbol{\xi}_1 = \boldsymbol{\xi}_0 + \Delta\boldsymbol{\xi}$ is found following the considerations reported below. Ignoring the quadratic contribution for sufficiently small $\Delta\boldsymbol{\xi}$, we have

$$Y_1^0 + ((\nabla Y_1)^0, \Delta\boldsymbol{\xi}) = 0, \tag{4.4}$$

where brackets denote scalar product. Taking into account that $(\nabla \tilde{W})^0$ determines the direction of a maximal increase in $\tilde{W}(\boldsymbol{\xi}, \mathbf{z})$ function at point $\boldsymbol{\xi} = \boldsymbol{\xi}_0$, we search for vector $\Delta\boldsymbol{\xi}$ in the form

$$\Delta\boldsymbol{\xi} = -t(\nabla \tilde{W})^0 + \zeta(\nabla Y_1)^0, \tag{4.5}$$

where t is a small parameter and ζ is an unknown value. Substituting Eq. (4.5) into Eq. (4.4), we finally arrive at

$$\Delta\boldsymbol{\xi} = -\left[(\nabla \tilde{W})^0 - \frac{((\nabla Y_1)^0, (\nabla \tilde{W})^0)}{((\nabla Y_1)^0)^2}(\nabla Y_1)^0\right]t - \frac{Y_1^0}{((\nabla Y_1)^0)^2}(\nabla Y_1)^0. \tag{4.6}$$

The optimal choice of parameter t is a complicated task. Too small or too large value of this parameter lead to a large number of iterations and, hence, to a slow convergence of the iteration method. One can use t value obtained at the preceding step, try to increase or decrease this value, and decide based on the results obtained, whether it is necessary to modify this value. This procedure is repeated until the corrections to the $\boldsymbol{\xi}$ value become sufficiently small. Then, one can pass to the minimization of $\tilde{W}$ using the Lagrange multiplier method.

5. DEPENDENCE OF MICELLE CHARACTERISTICS ON AGGREGATION NUMBERS AND SOLUTION CONCENTRATION UPON THE TRANSITION FROM SPHERICAL TO GLOBULAR AND CYLINDRICAL MODIFICATIONS OF MICELLES

When performing numerical calculations, we used three sets of initial parameters of a model. These sets differ from each other only in dipole moment p of the head group of surfactant molecule, i.e., according to Eq. (3.1), they differ in the values of dimensionless parameter κ. The obtained results were compared with analogous results for the model of conventionally spherical aggregate. The model of conventionally spherical aggregate was assumed to be the molecular aggregate whose shape is spherical at any aggregation number even when the packing condition can be violated. Physically, the micelle with the same aggregation number containing solubilizate could correspond to such an aggregate at $n > n^{(sp)}$. In such a situation, the aggregation work is determined by formula (2.12); moreover, from the thermodynamic meaning of the W_n value as a minimal work and the inapplicability of packing condition to the model of conventionally spherical aggregate, it follows that

$$W_n^{(sp)} \le \min(W_n^{(glob)}, W_n^{(cyl)}). \tag{5.1}$$

Hereafter in this paragraph, values referred to globular, cylindrical, and conventionally spherical aggregates are denoted by superscripts (glob), (cyl), and (sp), respectively.

We consider first the situation for spherical micelles studied in [11]. In this case, we deal with the following set of initial parameters of a model:

$$n_C = 18, \quad \varepsilon_p = 30, \quad \gamma = 30 \text{ mN/m}, \quad s_0 = v/l_C = 21 \text{ Å}^2, \quad p = 14.42 \text{ D}, \quad \delta = 3 \text{ Å}, \quad T = 293 \text{ K}. \tag{5.2}$$

With such choice of parameters, we have

$$n^{(sp)} = 117, \quad \kappa = 10.89. \tag{5.3}$$

Correspondingly, to find the aggregation work at $n < 117$, we take advantage of formula (2.12); at $n > 117$, the problem is to be solved numerically. According to the meaning of dimensionless parameter κ mentioned in Section 3 and the estimate of the electrostatic contribution to the aggregation work of spherical micelle with the radius of hydrocarbon core $R_m = l_C$, we conclude that, in the case under consideration, at $\kappa = 10.89$ and $n = n^{(sp)}$, we have $W_s < W_{el}$. Thus, the role of electrostatic contribution to the aggregation work in the transition region from spherical to nonspherical micelles is significant, although this contribution amounts only to 0.2 of hydrophobic contribution.

Results corresponding to this case are shown in Fig. 3. Total aggregation work W_n expressed in k_BT units is plotted on the ordinate. The analysis of Fig. 3 demonstrates that inequality (5.1) is fulfilled. Comparing $W_n^{(glob)}$ and $W_n^{(cyl)}$, we disclose that, at aggregation numbers $117 < n < 210$, the formation of globular micelles is more favorable; in the $n > 210$ region, spherocylindrical micelles are formed preferably. This situation corresponds to experimental observations: globular micelles dominate among small micelles; as the aggregation number increase, spherocylindrical micelles begin to dominate. Note in conclusion that, at $n \longrightarrow n^{(sp)} + 0$, all curves are merged into one; i.e., both the globular and spherocylindrical aggregates tend to acquire a spherical shape.

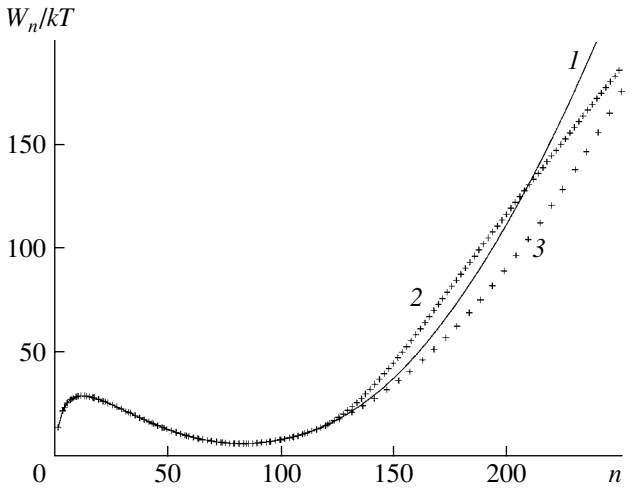

Fig. 3. The formation work of (*1*) globular, (*2*) spherocylindrical, and (*3*) spherical aggregates as a function of aggregation numbers at $\kappa = 10.89$ and $c_1/c^{\alpha} = 6.73 \times 10^{-8}$.

In the example shown in Fig. 3, the maximum and minimum of aggregation work fell into the $n < n^{(sp)}$ region. Consequently, aggregates with $n > n^{(sp)}$, in practice do not affect the character of direct and back transitions of aggregates over the maximum of aggregation work; therefore, it seems interesting to consider the case when the minimum of aggregation work lie deliberately in the $n > n^{(sp)}$ region. Choosing dipole moment p such that the inflection point of function (2.12) practically coincides with $n^{(sp)}$, we have

$$p = 9.34 \text{ D}, \quad \kappa = 4.57, \tag{5.4}$$

with the $n^{(sp)}$ value remaining the same ($n^{(sp)} = 117$). Estimating the electrostatic contribution for the spherical micelle with the radius of hydrocarbon core $R_m = l_C$, we arrive at $W_{el} \approx (1/2)W_s$. Hence, the electrostatic contribution to the aggregation work in the region of transition from spherical to nonspherical micelles is again not small.

Results corresponding to this case are shown in Fig. 4. Total aggregation work W_n expressed in k_BT units is plotted on the ordinate. It is seen that, in the $n > n^{(sp)}$ region, results obtained analytically for conventionally spherical aggregate noticeably differ from the data of numerical calculation for $W_n^{(glob)}$ and $W_n^{(cyl)}$. Such a discrepancy of these results is not surprising, because the model of conventionally spherical aggregate does not take packing conditions into account. In this case, inequality (5.1) is still fulfilled. As $n \longrightarrow n^{(sp)} + 0$, all curves are merged; i.e., both the globular and spherocylindrical micelles tend to acquire spherical shape (we remind to the reader that the initial numerical approximation for spherocylindrical micelles has the shape of long cylinder with hemispherical ends; for globules, the shape of sphere noticeably flattened at the poles).

Comparing $W_n^{(glob)}$ and $W_n^{(cyl)}$ in Fig. 4, we see that the minimum of aggregation work on curve $W_n^{(cyl)}$ lies much higher than that on curve $W_n^{(glob)}$. In general, in the $n^{(sp)} < n < 260$ region, the formation work of globular aggregates is smaller than that of spherocylindrical micelles; on the contrary, in the $n > 260$, the formation work of globular aggregates is larger. Hence, we conclude again that, globular micelles prevail among smaller aggregates; spherocylindrical micelles begin to dominate with an increase in aggregation numbers. Note that the position of globules–spherocylinders transition on the aggregation number axis does not depend on surfactant monomer concentration c_1. As will be shown later, the linear part of curve $W_n^{(cyl)}$ corresponds to the asymptotic of aggregation work for cylindrical micelles, and a sharp rise of this curve at $n > 300$ is related to the formation of voids inside the aggregate. Seemingly, such a behavior is explained by the insufficient accuracy of calculations (at a given number of series terms in expansion (3.6) of micelle profile) and the violation of the local packing condition.

Figures 5 and 6 present the characteristic profiles of spherocylindrical and globular micelles at various aggregation numbers and $\kappa = 4.57$. As should be expected, spherocylindrical micelles are tend to draw into an infinite cylinder, while globular micelles tend to transform into disc-like micelles or extended bilayers. This allows us to find $(dW_n^{(cyl)}/dn)_{as}$ and $(dW_n^{(glob)}/dn)_{as}$ asymptotics of the derivative of aggregation work for cylindrical and disc-like micelles, respectively. From Eqs. (3.2) and (2.14), for cylindrical micelle at $1/R_1 = 0$ and $1/R_2 = 1/l_C$, we obtain

$$\left(\frac{dW_n^{(cyl)}}{dn}\right)_{as} = \frac{2\gamma v}{l_C}\left(1 + \frac{\kappa}{4}\right) - b_2 \tag{5.5}$$

and, similarly, for disc-like micelle at $1/R_1 = 1/R_2 = 0$, we find

$$\left(\frac{dW_n^{(glob)}}{dn}\right)_{as} = \frac{\gamma v}{l_C}(1 + \kappa) - b_2. \tag{5.6}$$

Analyzing relations (5.6) and (5.5), we see that, at $\kappa < 2$ and large aggregation numbers, the globular shape of a micelle is thermodynamically more favorable than cylindrical; at $\kappa > 2$, the situation is reversed. This means that the electrostatic contribution significantly affects the micellization processes and, hence, it cannot be ignored. This effect is especially pronounced at $\kappa > 2$. Earlier, the role of large electrostatic contributions to the aggregation work of nonspherical micelles was not studied.

Equilibrium distributions of spherocylindrical and globular micelles over aggregation numbers should obey Boltzmann's principle and be proportional to

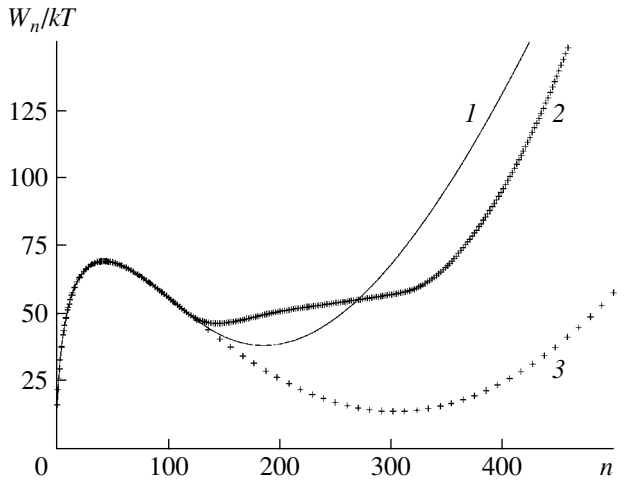

Fig. 4. The formation work of (*1*) globular, (*2*) spherocylindrical, and (*3*) spherical aggregates as a function of aggregation numbers at $\kappa = 4.57$ and $c_1/c^{\alpha} = 1.82 \times 10^{-9}$.

$\exp(-W_n^{(\mathrm{cyl})}/k_\mathrm{B}T)$ and $\exp(-W_n^{(\mathrm{glob})}/k_\mathrm{B}T)$ [16]. In order for these distributions to correspond the equilibrium state of micellar solution with finite surfactant amount, we set

$$\left(\frac{dW_n^{(\mathrm{cyl})}}{dn}\right)_{\mathrm{as}} > 0 \qquad (5.7)$$

and

$$\left(\frac{dW_n^{(\mathrm{glob})}}{dn}\right)_{\mathrm{as}} > 0. \qquad (5.8)$$

Evidently, conditions (5.7) and (5.8) at fixed set of model parameters, impose the upper bound of the surfactant concentration in solution. Considering again Figs. 3 and 4, we can see that conditions (5.7) and (5.8) are satisfied for these figures.

Accounting for Eq. (2.13), we rewrite conditions (5.5) and (5.6) as

$$\left(\frac{dW_n^{(\mathrm{cyl})}}{dn}\right)_{\mathrm{as}} = \frac{2\gamma v}{l_\mathrm{C}}\left(1 + \frac{\kappa}{4}\right) - Bn_\mathrm{C} - s_0\gamma - k_\mathrm{B}T\ln\frac{c_1}{c_\alpha}, \qquad (5.9)$$

$$\left(\frac{dW_n^{(\mathrm{glob})}}{dn}\right)_{\mathrm{as}} = \frac{\gamma v}{l_\mathrm{C}}(1 + \kappa) - Bn_\mathrm{C} - s_0\gamma - k_\mathrm{B}T\ln\frac{c_1}{c_\alpha}. \qquad (5.10)$$

At $\kappa = 4.57$, we have inequality $(dW_n^{(\mathrm{cyl})}/dn)_{\mathrm{as}} < (dW_n^{(\mathrm{glob})}/dn)_{\mathrm{as}}$; hence, condition (5.7) ensures the fulfillment of condition (5.8). With allowance for Eq. (5.9), the values of parameters γ, n_C, s_0, and T taken from (5.2) and $B = 1.4k_\mathrm{B}T$, condition (5.7) is true at

$$c_1/c^{\alpha} \le 2.1 \times 10^{-9}. \qquad (5.11)$$

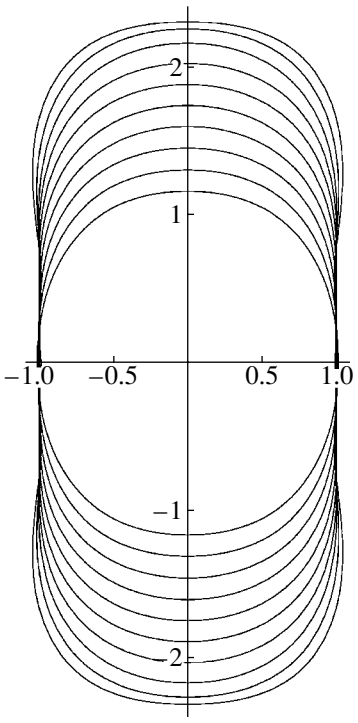

Fig. 5. Profiles of spherocylindrical micelle at $\kappa = 4.57$ and various aggregation numbers $n = 150 + 25m$, $m = 0, 1, \ldots, 9$.

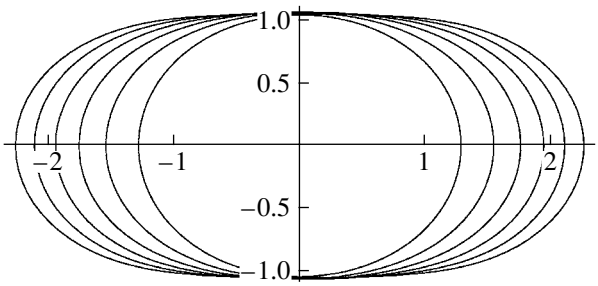

Fig. 6. Profiles of globular micelle at $\kappa = 4.57$ at various aggregation numbers $n = 200 + 100m$, $m = 0, 1, \ldots, 5$.

Figure 7 shows the positions of extreme points for the formation work of globular, spherocylindrical, and spherical aggregates in the aggregation number axis as a function of surfactant monomer concentration in the concentration range satisfying condition (5.11). The lower branch of curve *3* corresponds to the position of the first maximum of aggregation work for spherical aggregates (to aggregation number n_c for critical aggregate [11]); the upper branch, to the position of a minimum in the model of conventionally spherical aggregate (to aggregation number n_s for a stable aggregate [11]). Curve *1* corresponds to the positions of a minimum of aggregation work for globular aggregates. Specific trend of curve *2* is related to the fact that, as monomer concentration increases, only the position of a minimum for spherocylindrical aggregates corresponds first

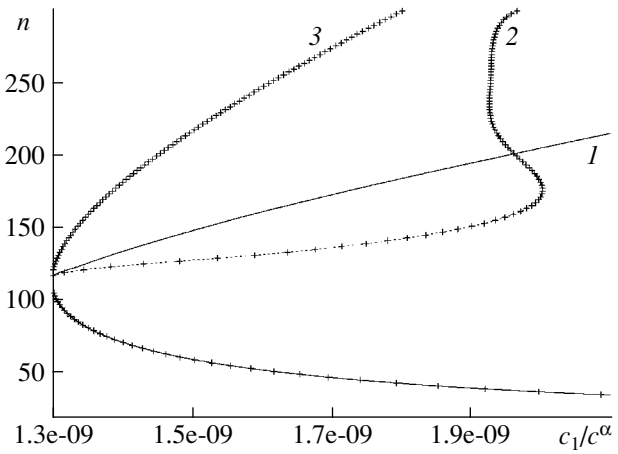

Fig. 7. Positions of extreme points of aggregation work for (*1*) globular, (*2*) spherocylindrical, and (*3*) spherical aggregates on the aggregation number axis as a function of surfactant monomer concentration at $\kappa = 4.57$.

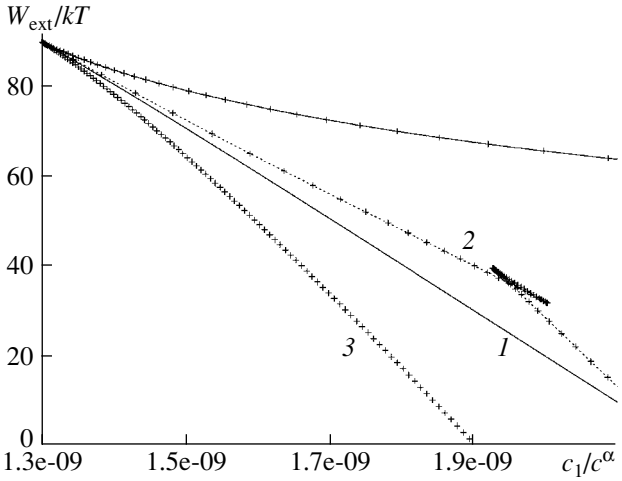

Fig. 8. Extreme point W_{ext} of aggregation work W_n for (*1*) globular, (*2*) spherocylindrical, and (*3*) spherical aggregates as a function of surfactant monomer concentration at $\kappa = 4.57$.

to this curve; beginning with a certain monomer concentration, both the positions of the second maximum and second minimum of aggregation work for spherocylindrical aggregates. More details will be reported in the next section. We note once again that conventionally spherical model is poorly suitable for describing micelles at $n > n^{(sp)}$.

Figure 8 presents extreme points W_{ext} of aggregation work W_n for globular, spherocylindrical, and spherical aggregates as a function of surfactant monomer concentration. The upper branch of curve *3* corresponds to the height of the first maximum of aggregation work for spherical aggregates (to the W_c value of aggregation work for critical aggregate [11]); the lower curve, to the depth of minimum in the model of conventionally spherical aggregate (to the W_s value of the aggregation work for stable aggregate). Curve *1* corresponds to the depth of a minimum of aggregation work for globular aggregates. Specific trend of curve *2* is related to the fact that, as monomer concentration increases, only the depth of a minimum for spherocylindrical aggregates corresponds first to this curve; beginning with a certain monomer concentration, both the height of the second maximum and the depth of the second minimum of aggregation work for spherocylindrical aggregates appear in this curve.

Finally, let us consider the third interesting case when, at $\kappa < 2$ and in accordance with the preceding, the role of globular micelles should rise. Using condition (5.8) of positive asymptotics for disc-like micelles, assuming that the maximum of aggregation work lies in the region of spherical molecular aggregates and accounting for Eqs. (2.12), (2.13), and definition of parameter κ in (3.1), we come to conclusion that permissible κ values fall on interval $1.8 \le \kappa < 2$. Therefore, we choose $\kappa = 1.9$.

The plot of aggregation work corresponding to this case is presented in Fig. 9. As is seen from the ratio between the depths of minima in the plot, in this case, only globular and disk-like micelles will be predominantly present in the solution; the fraction of spherocylindrical micelles will be negligible. At chosen values of model parameters and monomer concentration, in view of condition (5.10), the asymptotic of aggregation work for globular micelles should virtually be horizontal; however, an increase in aggregation work is observed in Fig. 9 at $n > 1200$. An increase in the number of terms in expansion (3.6) of micelle profile leads to a decrease in the positive slope of the plot in this region. Thus, the observed growth of aggregation work is related to the inadequate accuracy of calculations at large aggregation numbers.

6. CONDITIONS OF THE EXISTENCE OF THE SECOND MAXIMUM OF AGGREGATION WORK

The presence of the second maximum on the dependence of aggregation work on the aggregation number of surfactant molecules in the transition region to spherocylindrical micelles is often associated with the existence of the second micellization concentration (second CMC) in the solutions of corresponding surfactants [13, 16]. The first CMC is usually determined as the surfactant concentration in solution at which the amount of substance in a micellar phase (as a rule, spherical micelles) comprises a noticeable portion (about 10%) of the total amount of a surfactant. Evidently, this takes place when the first maximum on the curve of aggregation work and the barrier needed for the transition to spherical micelles are lowered to a fairly high degree. By analogy with this definition, the second CMC can be introduced at which about 10% of the total amount of surfactant is accumulated but in

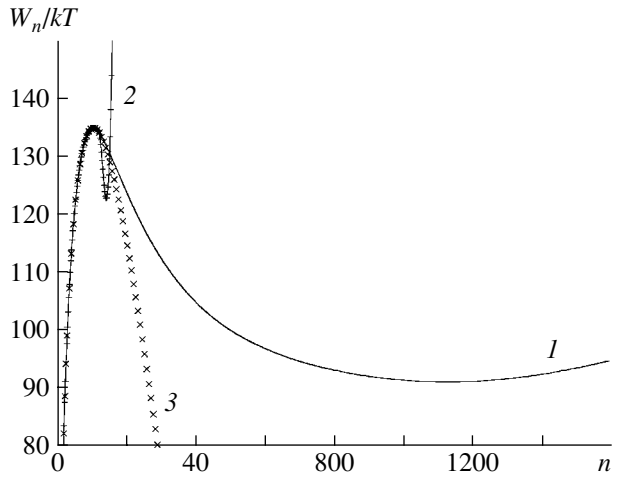

Fig. 9. The formation work of (*1*) globular, (*2*) spherocylindrical, and (*3*) spherical aggregates as a function of aggregation numbers at $\kappa = 1.90$ and $c_1/c^\alpha = 2.22 \times 10^{-10}$.

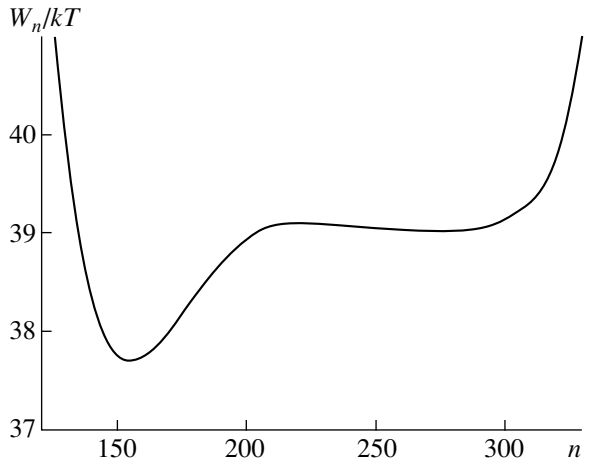

Fig. 10. The aggregation work for spherocylindrical aggregate as a function of aggregation numbers at $\kappa = 4.57$ and surfactant monomer concentration $c_1/c^\alpha = 1.93 \times 10^{-9}$ at which the second maximum of work becomes noticeable.

cylindrical micelles [16]. With the existence of the second maximum on the curve of aggregation work at aggregation numbers corresponding to the transition to spherocylindrical micelles, this maximum (to be more exact, the difference between the second maximum and the first minimum of aggregation work) will be small enough so that the transition from spherical to spherocylindrical micelles can occur with high probability. In particular, this can be achieved at surfactant monomer concentrations in solution, at which aggregation work of spherocylindrical micelles is characterized by a positive asymptotic (5.5) approaching zero.

As is seen from Figs. 7 and 8, curve $W_n^{(\mathrm{cyl})}$ at a certain value of parameters can have the second maximum and even the second minimum, in addition to the first maximum of aggregation work in the region of spherical aggregates. These facts explain the specific features of curve trends in these figures for spherocylindrical aggregates (additional inflection in Fig. 7 and additional break in Fig. 8) in the range of surfactant monomer concentration of $1.92 \times 10^{-9} < c_1/c^\alpha < 2.00 \times 10^{-9}$. According to Eqs. (5.9) and (5.11), at such concentrations, the slope of asymptotic of the aggregation work for spherocylindrical micelles is indeed close to zero.

This is shown in more detail in Fig. 10 at surfactant monomer concentration $c_1/c^\alpha = 1.93 \times 10^{-9}$. The region of aggregation numbers corresponding to the transition to spherocylindrical micelles is enlarged in this figure. The first minimum and the second maximum of aggregation work for the aggregates transforming into spherocylindrical micelles are well seen. The second minimum in Fig. 10 is quite indistinguishable. However, it is distinctly seen in Fig. 11 for the derivative of aggregation work with respect to aggregation numbers. Figure 11 demonstrates that the $dW_n^{(\mathrm{cyl})}/dn$ plot twice intersects the abscissa axis. The first intersection corresponds to the position of second maximum and the second intersection, to that of the second minimum of aggregation work. Nonzero (albeit small positive) asymptotic $(dW_n^{(\mathrm{cyl})}/dn)_{\mathrm{as}} \approx 0.0015 k_\mathrm{B}T$ corresponds to the case presented in Figs. 10 and 11. With the existence of the second maximum and the second minimum, the derivative of aggregation work with respect to aggregation numbers should achieve its asymptotic from the side of lower values. However, the derivative of aggregation work in Fig. 11 tends to asymptotic from below and then increases at $n > 270$. Such a behavior is explained by the inadequate accuracy of calculations and the violation of local packing condition at large aggregation numbers.

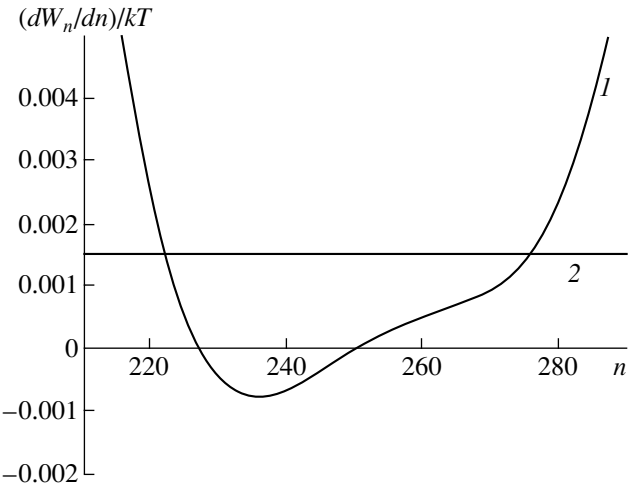

Fig. 11. The derivative of aggregation work with respect to aggregation numbers for (*1*) spherocylindrical aggregate and (*2*) its asymptotic form as a function of aggregation numbers at $\kappa = 4.57$ and $c_1/c^\alpha = 1.93 \times 10^{-9}$. The first and second zeros of the derivative of aggregation work correspond to the positions of the second maximum and the second minimum of aggregation work, respectively.

CONCLUSIONS

The considered approach made it possible to analyze, within the framework of the droplet model of nonionic surfactant molecular aggregates, two equilibrium branches of the curve of aggregation work for nonspherical micelles. One of these branches corresponds to globular, while the other, to spherocylindrical micelles. Both curves significantly differ from the result obtained within the framework of conventionally spherical molecular aggregate ignoring the condition of monomer packing into a micelle. This difference is exhibited most distinctly in the situation when the minimum of aggregation work lies beyond the domain of applicability of spherical packing. Regardless of the fact that numerical starting approximations of aggregate profiles were taken as nonspherical, globular, and spherocylindrical aggregates, they are transformed into the limiting sphere at the aggregation numbers corresponding to the limiting spherical packing.

We studied the role of electrostatic contribution to the aggregation work for nonspherical micelle and demonstrated that this role is determined by the dimensionless parameter κ characterizing the ratio of electrostatic and surface contributions to the aggregation work at the limiting radius of spherical packing. At $\kappa > 2$ and aggregation numbers slightly exceeding the limit of spherical packing, the formation of globular micelles is thermodynamically more favorable than the formation of spherocylindrical aggregates. As the aggregation number increases further at $\kappa > 2$, the formation of spherocylindrical micelles becomes preferable. At $\kappa < 2$, the formation of globular micelles transforming into disc-like micelles is thermodynamically more advantageous throughout the range of aggregation numbers exceeding the limit of spherical packing.

It was elucidated that, at certain values of model parameters and surfactant monomer concentration in solution, the second maximum appears on the curve of aggregation work of spherocylindrical micelles as a function of aggregation numbers. The appearance of the second maximum, in addition to the maximum in the region of submicellar aggregates for spherical micelles, is due to the sum of surface and electrostatic contributions to the aggregation work and is not related to the conformational contribution.

Although the second maximum on the curve of aggregation work in the region of spherocylindrical micelles was also discussed in [13], its nature was not quite cleared in the cited work. The model of spherocylinder composed of two spherical segments with radius $R_m = l_C$ and connecting neck was studied in [13]. All parameters for spherical segments were calculated analytically, and the neck shape was found from the conditions of minimum of aggregate formation work and the absence of breaks. In this case, conformational contribution W_n^d of $W_n^d = \tau_d \int (b - b^*)^2 dn'$ type, where b is the radius of micelle cylindrical segment, b^* is its optimal value, τ_d is the deformation coefficient of hydrocarbon tails, and n' is the number of molecules in cylindrical segment, was added to surface and electrostatic (1.16) contributions. In this model, parameter b^* is an adjustment parameter. For better agreement with experimental data, May and Ben-Shaul used $b^* \approx 0.8 l_C$. At such an approach, radius b tends to its optimal value. Because of this, $b < l_C$; hence, the packing conditions are always fulfilled. Therefore, the account of conformational contribution in [13] was significant. However, as was shown in our calculations, the second maximum exists also even when the conformational contribution can be ignored at the background of hydrophobic contribution.

ACKNOWLEDGMENTS

This work was supported by the Russian Foundation for Basic Research, project no. 04-03-32134.

REFERENCES

1. Tanford, C., *J. Phys. Chem.*, 1974, vol. 78, p. 2469.
2. Tanford, C., *The Hydrophodic Effect: Formation of Micelles and Biological Membranes*, Toronto: Wiley, 1980.
3. Israelachvili, J.N., Mitchel, D.J., and Ninham, B.W., *J. Chem. Soc., Faraday Trans. 2*, 1976, vol. 72, p. 1525.
4. Nagarajan, R. and Ruckenstein, E., *J. Colloid Interface Sci.*, 1977, vol. 60, p. 221.
5. Nagarajan, R. and Ruckenstein, E., *J. Colloid Interface Sci.,* 1979, vol. 71, p. 580.
6. Nagarajan, R. and Ruckenstein, E., *J. Colloid Interface Sci.*, 1983, vol. 91, p. 500.
7. Rusanov, A.I., *Zh. Vses. Khim. O–va im. D.I. Mendeleeva,* 1989, vol. 34, no. 2, p. 174.
8. Nagarajan, R. and Ruckenstein, E., *Langmuir*, 1991, vol. 7, p. 2934.
9. Rusanov, A.I., *Mitselloobrazovanie v rastvorakh poverkhnostno-aktivnykh veshchestv* (Micellization in Surfactant Solutions), St. Petersburg: Khimiya, 1992.
10. Nagarajan, R., in *Structure-Performance Relationships in Surfactants*, Esumi, K. and Ueno, M., Eds., New York: Marcel Dekker, 1997, p. 1.
11. Rusanov, A.I., Kuni, F.M., Grinin, A.P., and Shchekin, A.K., *Kolloidn. Zh.*, 2002, vol. 64, p. 670.
12. Rusanov, A.I., Grinin, A.P., Kuni, F.M., and Shchekin, A.K., *Zh. Obshch. Khim.,* 2002, vol. 72, p. 651.
13. May, S. and Ben-Shaul, A., *J. Chem. Phys.*, 2001, vol. 105, p. 630.
14. Vodnev, V.T., Naumovich, A.F., and Naumovich, N.F., *Osnovnye matematicheskie formuly. Spravochnik* (Fundamental Mathematical Formulae: A Handbook), Bogdanov, Yu.S., Ed., Minsk: Vysheishaya Shkola, 1995.
15. Dennis, J., Jr. and Schnabel, R., *Numerical Methods for Unconstrained Optimization and Nonlinear Equations*, Englewood Cliffs: Prentice Hall, 1983.
16. Kuni, F.M., Shchekin, A.K., Rusanov, A.I., and Grinin, A.P., *Kolloidn. Zh.*, 2004, vol. 66, p. 204.